Probing pH-Dependent Functional Elements in Proteins: Modification of Carboxylic Acid Pairs in *Trichoderma reesei* Cellobiohydrolase Cel6A†

Gerd Wohlfahrt,‡ Tarmo Pellikka,§ Harry Boer,§ Tuula T. Teeri,|| and Anu Koivula*,§

Orion Pharma, P.O. Box 65, FIN-02101 Espoo, Finland, VTT Biotechnology, P.O. Box 1500, FIN-02044 VTT, Finland, and Royal Institute of Technology, Department of Biotechnology, S-10691 Stockholm, Sweden

Received June 3, 2003

ABSTRACT: Two carboxylic acid side chains can, depending on their geometry and environment, share a proton in a hydrogen bond and form a carboxyl−carboxylate pair. In the *Trichoderma reesei* cellobiohydrolase Cel6A structure, five carboxyl−carboxylate pairs are observed. One of these pairs (D175-D221) is involved in catalysis, and three other pairs are found in, or close to the two surface loops covering the active site tunnel of the catalytic domain. To stabilize Cel6A at alkaline pH values, where deprotonation of the carboxylic acids leads to repulsion of their side chains, we designed two mutant enzymes. In the first mutant, one carboxyl−carboxylate pair (E107-E399) was replaced by a corresponding amide-carboxylate pair (Q107-E399), and in the second mutant, all three carboxyl−carboxylate pairs (E107-E399, D170-E184, and D366-D419) were mutated in a similar manner. The unfolding studies using both intrinsic tryptophan fluorescence and far-ultraviolet circular dichroism spectroscopy at different pH values demonstrate that the unfolding temperature (T_m) of both mutants has changed, resulting in destabilization of the mutant enzymes at acidic pH and stabilization at alkaline pH. The effect of stabilization seems additive, as a Cel6A triple mutant is the most stable enzyme variant. This increased stability is also reflected in the 2- or 4-fold increased half-life of the two mutants at alkaline pH, while the catalytic rate on cellotetraose (at $t = 0$) has not changed. Increased operational stability at alkaline pH was also observed on insoluble cellulosic substrates. Local conformational changes are suggested to take place in the active site loops of Cel6A wild-type enzyme at elevated pHs (pH 7), affecting to the end-product spectrum on insoluble cellulose. The triple mutant does not show such pH-dependent behavior. Overall, our results demonstrate that carboxyl−carboxylate pair engineering is a useful tool to alter pH-dependent protein behavior.

Enzymes and other proteins are used in a broad range of biotechnical and biomedical applications, for example, in diagnostics (antibodies), as drug molecules (hormones), or as catalysts (amylases, proteases, cellulases) in chemical processes. Several potential applications are, however, hampered by the low stability of proteins under process conditions. Key objectives in industrial applications are stability at high temperature and resistance against chemical denaturants, oxidation, and proteolysis. Nowadays, there are two main protein engineering approaches to address these questions: directed evolution and rational (structure based) protein design. Results from those studies have confirmed the dominating influence of hydrophobic interactions in the core of a protein structure but have also revealed the nonnegligible role of electrostatic interactions and hydrogen bonds. Recent work demonstrates also the importance of charge−charge interactions on the protein surface (*1*).

The existence of carboxyl−carboxylate interactions in proteins and their possible effect on protein stability was discussed in the literature for the first time 20 years ago (*2*). The occurrence of these carboxyl−carboxylate pairs in protein structures from the Protein Data Bank (*3*) has later been analyzed in a systematic approach, which led to a suggestion of their importance in enzyme catalysis and binding of substrates (*4*). Experimental work by Mortensen and Breddam (*5*) showed that the stability of a serine carboxypeptidase was significantly decreased by removal of a pair of glutamic acids in the active center of the enzyme. This destabilizing effect was strongest at low pH values.

On the other hand, it has been proposed that low-barrier hydrogen bonds (LHBH)[1] might play a role in enzymatic catalysis (see Cleland et al. for a review) (*6*). Although it is still under debate whether LBHBs really exist in proteins, there is experimental evidence that short hydrogen bonds in proteins can be stronger than those of normal length (*6*). In

† This work was funded by the European Commission (Biotechnology Program DG XII Project BIO4-CT96-0580) and the Academy of Finland.

* To whom correspondence should be addressed. Fax: +358-9-455 2103. E-mail: Anu.Koivula@vtt.fi.

‡ Orion Pharma.

§ VTT Biotechnology.

|| Royal Institute of Technology.

[1] Abbreviations: BMCC, bacterial microcrystalline cellulose; CBD, cellulose-binding domain (module); GuHCl, guanidium hydrochloride; HEC, hydroxyethyl cellulose; LBHB, low-barrier hydrogen bond; MeUmb(Glc_1), 4-methylumbelliferyl-β-D-glucopyranoside; MeUmb-($Glc)_2$, 4-methylumbelliferyl-β-D-cellobioside; NaAc, sodium acetate; PAHBAH, *p*-hydroxylbenzoic acid hydrazine; PDB, Protein Data Bank; SDS, sodium dodecylsulphate.

10.1021/bi034954o CCC: $25.00
Published on Web 08/08/2003

general, the strength of a hydrogen bond depends on its length and linearity, its microenvironment (ligands and solvation), and how well the pK_a values of the conjugated acids match. With respect to these factors, pairs of carboxylic acid side chains in proteins could meet the criteria to form strong or some even low-barrier hydrogen bonds.

In the present paper, we show that engineering carboxyl−carboxylate pairs forming hydrogen bonds can be used to enhance stability of a fungal cellulase, Cel6A. The theoretical background to this study is described in detail elsewhere (G. Wohlfahrt, manuscript in preparation). Cel6A is one of the two major cellobiohydrolases secreted by the industrially important mesophilic fungus *Trichoderma reesei*. *Trichoderma* cellobiohydrolases are enzymes that are most efficient on highly crystalline cellulose. They produce mainly cellobiose from the chain ends in a processive manner catalyzing several consecutive bond cleavages before dissociating from the substrate (*7*−*10*). Both *T. reesei* cellobiohydrolases are composed of a separate catalytic module and of a cellulose-binding module, joined together by a long glycosylated linker (*7*). Crystal structures of the catalytic module (domain) of *T. reesei* Cel6A wild-type and various mutants in complex with different ligands have been described (*8*, *11*, *12*). The active site of Cel6A is formed by surface loops, and it provides binding sites for six glucosyl units; four of these binding sites (−2 → +2) are buried in a tunnel going through the catalytic domain (*11*). The catalytic domain of Cel6A belongs to the glycosyl hydrolase family 6, from which more than 60 different sequences are found in the CAZy database (*13*) (http://afmb.cnrs-mrs.fr/CAZY/acc.html) and detailed 3-D structures have been described for four different cellulases of fungal and bacterial origin.

All potent cellulolytic microorganisms secrete a battery of cellulolytic enzymes, which cleave the *O*-glycosidic linkage of a cellulose chain by an acid hydrolysis mechanism. *T. reesei* Cel6A functions optimally under acidic pH; its pH optimum being between pH 4−6 (*14*). The published pH optima of various family 6 cellulases range from pH 4 to 9. We were interested in identifying structural motifs responsible for stability in the neutral or alkaline pH range and whether *T. reesei* Cel6A could be engineered to function like the more alkalophilic cellulases in this family.

EXPERIMENTAL PROCEDURES

Construction of the Mutant Clone and Transformation to T. reesei. Escherichia coli strain DH5α (Promega) was used as the cloning host for all the DNA constructions and *T. reesei* strain lacking the endogeneous genes for the endoglucanase Cel5A and the cellobiohydrolase Cel6A as the production host of the mutant enzymes. For selection of *Trichoderma* transformants, hygromycin selection plasmid pRLMex30 was used (*15*). The constructions of the mutant plasmids were done by PCR overlap extension method, and the mutated area was subjected to DNA sequencing. Mutations E107Q (GAA → CAA) and E107Q/D170N/D366N (GAA → CAA/GAC → AAC/GAC → AAC) were first introduced to the full length *cel*6A cDNA in pSP73 plasmid (Promega). The mutated cDNAs were then cloned under the *cel*7A (former *cbh1*) promoter of the fungal expression construction as described earlier (*14*). *Trichoderma* transformation and choosing the best producing transformant was performed basically as described by Ståhlberg et al. (*16*).

Protein Production and Purification. The Cel6A mutants were produced as described by Srisodsuk et al. (*17*) and purified essentially as described by Reinikainen et al. (*18*). Briefly, culture supernatants were separated from mycelia and concentrated. After desalting with Biogel P-6 (Bio-Rad, Cambridge, MA), the protein solutions were run through a DEAE-Sepharose FF column (Pharmacia, Uppsala, Sweden) equilibrated in 50 mM sodium acetate buffer (pH 5.6). The flow-through fractions containing Cel6A protein were further purified by thiocellobioside-based affinity chromatography (*19*). The purity of the mutant preparates were checked and verified by SDS−PAGE (*20*) and Western blotting (*21*). The presence of contaminating cellulolytic activities were ruled out by measuring the activities against MeUmb(Glc_1), MeUmb($Glc)_2$, and hydroxyethyl cellulose (HEC) as described earlier (*22*). Concentrations of purified wild-type and mutated proteins were determined from UV absorbance at 280 nm using the molar extinction coefficient $\epsilon = 104\,000$ M^{-1} cm^{-1} measured with total amino acid analysis for the intact Cel6A wild-type enzyme (A. Koivula, unpublished results).

Immunoreagents. For Western blot analysis, monoclonal antibodies CII-8 and CII-82 raised against Cel6A were used to detect Cel6A as described previously (*23*).

Measurement of Enzymatic Activity. Turnover numbers for the hydrolysis of cellotetraose (Glc_4) at 44 °C were determined by HPLC (Waters Millipore, Milford, MA) equipped with a refractive index (RI) detector as described earlier (*14*, *24*). The column used for separation of cello-oligosaccharides was Aminex HPX-42 A (Bio-Rad), and soluble cello-oligosacchrides (Glc_1−Glc_4) were used as standards. Turnover numbers were obtained from the initial velocities of the reaction curves by a nonlinear regression data analysis program (Origin). The substrate concentration in the reaction mixture was 300 μM, and the enzyme concentration was between 0.007 and 0.15 μM. At pH 5 and 7.7, activities were also determined at substrate concentrations of 600 and 90 μM to verify that 300 μM is a saturating substrate concentration. In all measurements, samples were taken at eight to 11 different time points. The following buffers were used: 50 mM sodium acetate, pH 5.0; 50 mM potassium phosphate, pH 6.1 and 7.1; 30 mM potassium phosphate, pH 7.7; and 50 mM glycine/NaOH, pH 9.0. Determination of the $t_{1/2}$ values was performed at 44 °C in 30 mM potassium phosphate, pH 7.7 and using 300 μM cellotetraose as the final substrate concentration.

Bacterial microcrystalline cellulose (BMCC) was prepared from Nata de Coco (Reyssons Food Processing, The Philippines) basically as described by Gilkes et al. (*25*). The enzymatic activity on BMCC was determined by shaking the intact enzymes (final concentration of 1.8 μM) and substrate (0.7 mg/mL) at 44 °C in 30 mM potassium phosphate, pH 7.5. Samples were taken at designated time points, and the reaction was stopped by adding half the reaction volume of a stop-reagent containing 9 vol of 94% ethanol and 1 vol of 1 M glycine, pH 11.2. Samples were filtered through Millex GV 0.22-μm units (Millipore). The soluble reducing sugars were assayed by *p*-hydroxybenzoic acid hydrazide (PAHBAH) reagent using a cellobiose standard curve according to Boer et al. (*26*).

The solvent regenerated, amorphous cellulose was prepared from Avicel (Fluka AG, Switzerland) as described by Isogai and Atalla (*27*). The enzymatic activity on amorphous cellulose was determined at pH 5.0 (50 mM NaAc) and pH 7.0 (50 mM potassium phosphate) as described above for BMCC hydrolysis taking duplicate or triplicate samples at each time point. Final enzyme concentration in the hydrolysis experiments was 1.4 μM, substrate concentration was 1.0 mg/mL, and the incubation temperature was 27 °C. Soluble sugars were analyzed by HPLC using cello-oligosaccharides as standards as previously described.

Fluorescence Measurements and Circular Dichroism Spectroscopy. Unfolding studies based on monitoring the intrinsic tryptophan fluorescence of Cel6A wild-type and the mutant proteins were performed on a Shimadzu RF-5000 spectrofluorometer using both guanidium hydrochloride and temperature as denaturants (*28*). Emission and excitation spectra were recorded with a bandwidth of 5 nm on both monochromators. A thermostated cuvette holder connected to a water bath controlled the temperature of the sample solution.

Guanidium hydrochloride was used to measure unfolding of the enzymes at pH 6 and 8 (*29*). A GuHCl stock solution (6 M) in 50 mM potassium phosphate buffer was diluted in 50 mM potassium phosphate buffer resulting in a two dilution series with an increasing amount of GuHCl (0−4 M). The pH of the two series of solutions was adjusted to pH 6 and 8 by adding 5 M NaOH, and the concentration of GuHCl in solution was determined by measuring the refractive index as described by Nozaki (*30*). Twenty μL of enzyme solution and 480 μL of GuHCl solution were mixed giving a final enzyme concentration of 1.0 μM. The pH 6 and 8 series were first incubated for 24 h at 22 °C, and the intrinsic fluorescence of the samples with an increasing amount of GuHCl was then measured at an excitation wavelength of 280 nm and an emission wavelength of 340 nm. All points of both series were measured at least in duplicates. The fraction of unfolded protein was calculated using the equation $f_u = (y - y_n)/(y_u - y_n)$; where f_u is unfolded fraction, y is fluorescence of sample, y_n is fluorescence of native sample, and y_u is the fluorescence of the unfolded sample. Reversibility of reaction was tested by incubating a sample for 2 or 4 h in GuHCl solution, diluting it 4-fold (1/4) to a buffer solution, and letting it stand for ≤24 h at room temperature, after which the fluorescence was measured. A sample diluted into GuHCl solution was used as a control.

Temperature-induced unfolding was monitored by heating samples gradually (approximately 1 °C/min) up to 80 °C and measuring the fluorescence intensity. The temperature of the sample solution was measured continuously using a Fluke 52 electronic thermometer equipped with a K-type thermocouple that was immersed in the solution. Intrinsic fluorescence of samples was recorded after every 0.5 °C by measuring the emission at 340 nm using an excitation wavelength of 280 nm. The change in the fluorescence intensity of the sample was plotted as a function of temperature, smoothed, and differentiated by using Origin graphics and data analyses software. The culmination point of each curve was taken as a unfolding temperature (T_m). All points were measured at least in duplicates. The buffers used were 50 mM citrate/HCl, pH 3.0; 50 mM glycine/HCl, pH 3.7; 50 mM sodium acetate, pH 5.0; 50 mM potassium phosphate, pH 6.0; 50 mM potassium phosphate, pH 7.1; 50 mM potassium phosphate, pH 7.9; and 50 mM sodium borate/HCl, pH 9.0. Enzyme concentration in the fluorescence experiments was invariably 0.5 μM.

CD measurements were performed on a Jasco J-720 CD spectrometer equipped with a PTC-38WI Peltier type temperature control system that controlled the temperature in the cuvette. Spectra were recorded from 240 to 190 nm (using a 1 mm cell and a bandwidth of 1 nm) every 5 °C and every 2.5 °C around the unfolding temperature (T_m) until a temperature of 80 °C was reached. The measurements were performed at pH 6.1 and 7.9 in a 10 mM potassium phosphate buffer, and the enzyme concentration in the CD experiments was 2.6−2.9 μM.

RESULTS AND DISCUSSION

Structural Analysis of Carboxyl−Carboxylate Pairs in Cel6A. A detailed structural analysis of the proteins deposited in the PDB (*3*) revealed that, in a subset of proteins sharing less than 90% sequence identity, 19% contain at least one pair of carboxylic acids having their side-chain oxygen atoms within hydrogen-bonding distance (G. Wohlfahrt, manuscript in preparation). As the distance between those interacting oxygen atoms is frequently very short (∼2.55 Å), many of these carboxylic acids are suggested to share a proton in a strong hydrogen bond, and some could even form a LBHB when situated in an appropriate structural environment (low dielectric constant). The pK_a values of these carboxyl−carboxylate pairs are expected to differ significantly from free or differently ligated aspartate or glutamate side chains in proteins. At very low pH values, both of the carboxylic acid side chains in a carboxyl−carboxylate pair are protonated, and a normal strength hydrogen bond is formed (Figure 1). At intermediate pH (around pH 3−6), a proton is shared between both carboxyl groups, and this is suggested to result in formation of a strong hydrogen bond. At high pH values, both carboxyl groups are negatively charged, and this leads to repulsion of the side chains (Figure 1). In contrast to a carboxyl−carboxylate pair, a corresponding amide−carboxylate pair can exist in only two different protonation states in physiological pH, and in both states a hydrogen bond can be formed (Figure 1). Below pH 4−5, the carboxylic acid side chain is protonated, which probably destabilizes the hydrogen bond because of weaker electrostatic interactions. Above pH 4−5, the conjugate base is charged, and a normal hydrogen bond is formed between the carboxylate and the amide groups.

Examination of the *T. reesei* Cel6A 3-D structures revealed five potential carboxyl−carboxylate pairs (E107-E399, E146-E208, D170-E184, D175-D221, and D366-D419) (Figure 2). For four of these pairs, a short distance between their interacting carboxyl oxygens (2.5 ± 0.1 Å) is seen in all published X-ray structures (Table 1). The pair E146-E208 is not conserved among family 6 enzymes (Figure 3), and its side-chain oxygens are not equally close to one another in different X-ray structures and may thus not be hydrogen bonded. Further, the short distance of 2.94 Å in 1QJW (chain B) seems to be promoted by an interaction with a common ligand, such as a cadmium atom. Of the remaining four carboxyl−carboxylate pairs, D175-D221 is composed of the key catalytic residues of the enzyme and is strictly conserved

Table 1: Structural Features of Carboxyl−Carboxylate Pairs in Cel6A (1QK2 Chain A)

carboxyl−carboxylate pair	E107-E399	D170-E184	D366-D419	D175-D221	E146-E208
O−O distance[a]	2.55 ± 0.08	2.57 ± 0.07	2.46 ± 0.11	2.53 ± 0.09	4.08 ± 1.58
geometry[b]	anti-syn	anti-syn	anti-syn	syn-syn	anti-anti[c]
interplanar (deg)[d]	61	48	134	154	148[c]
Cα temp-fact.	15.0/11.4	13.4/21.9	13.7/12.5	22.2/16.5	17.0/20.4
solv.-acc. (A^2)[e]	5.7	6.3	3.5	4.9	30.9
H-bonds with nonwater	substrate-analogue O6	L139 N		Y169 OH N225 ND	Cd[c]

[a] Average values and standard deviations are calculated from six Cel6A structures in the PDB (1CB2, 1HGW, 1HGY, 1QJW, 1QK0, and 1QK2). [b] Refers to the position of the hydrogen bond in the carboxyl−carboxylate pair relative to the oxygens that are not involved in hydrogen bond formation (see Figure 1). [c] Values are taken from PDB 1QJW chain B. [d] The interplanar angle between the two interacting carboxyl groups. [e] Sum of the solvent accessible area of the side-chain oxygens in the carboxyl−carboxylate pairs calculated with the PSA program (*37*) using a probe radius of 1.4 Å.

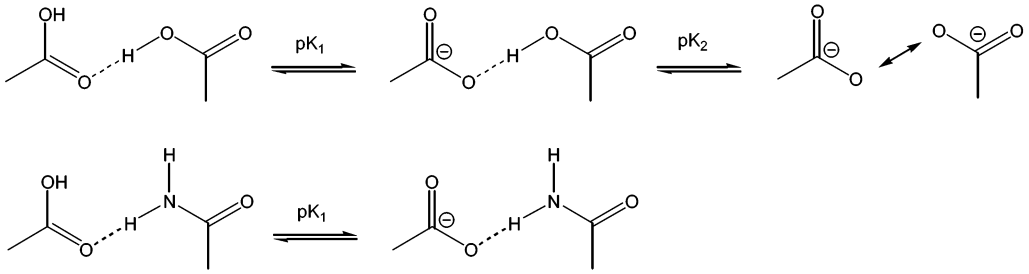

FIGURE 1: Schematic representation of different protonation states of carboxyl−carboxylate (top) and amide-carboxylate pairs (bottom) in the physiological pH range. The carboxyl−carboxylate pair is drawn so that the hydrogen bond is in the energetically favorable anti-syn geometry with respect to the noninteracting oxygen atoms. At intermediate pH (pH 3−6), a proton is shared between the two carboxyl groups, which could lead to the formation of a strong, LBHB-type hydrogen bond, in an appropriate structural environment. This would result in a carboxyl−carboxylate pair with three microscopic pK_a values, which combine to the two macroscopic pK_a values shown in the figure. In contrast, if a normal hydrogen bond is formed between the two carboxyl groups, the ionization equilibria of the two interacting acid−base groups involve four microscopic pK_a values (i.e., the pK_a of each group in the presence of a neutral or charged neighbor).

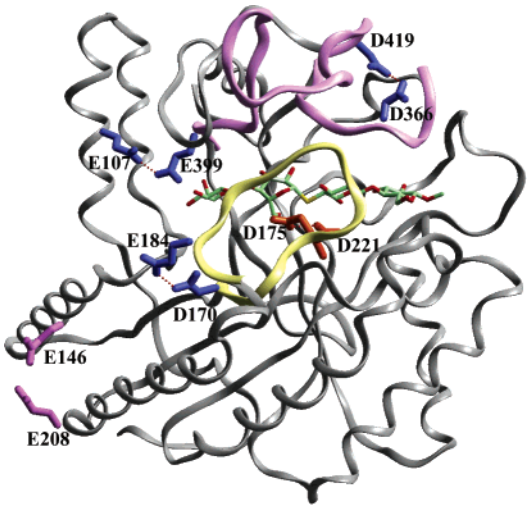

FIGURE 2: Location of the five putative carboxyl−carboxylate pairs in the *T. reesei* Cel6A catalytic domain. Coordinates are taken from the PDB (1QK2). The three pairs subjected to mutation are shown in blue and the catalytic acids in orange. Two loop regions covering the active-site tunnel, which is also indicated by a bound substrate analogue, are shown in yellow (Y169−S186) and violet (E399−W430).

within family 6 cellulases (*12*). The three other carboxyl−carboxylate pairs (E107-E399, D170-E184, and D366-D419) are not very well-conserved among the glycosyl hydrolase family 6 enzymes acting at neutral or alkaline pH values, such as *Humicola insolens* or *Thermobifida fusca* cellulases, whereas they seem to show a higher degree of conservation in enzymes with more acidic pH optima (Figure 3). This implies that they may have a role in stabilizing *T. reesei* Cel6A at low pH. The configuration of all three pairs in *T. reesei* Cel6A is anti-syn (Figure 1), which is the most frequent and probably the most stable spatial arrangement of pairs of carboxylic side chains in proteins. The solvent accessibility of all three carboxyl−carboxylate pairs is low (Table 1), which also seems to be a prerequisite for formation of this type of hydrogen bond (G. Wohlfahrt, manuscript in preparation). Further structural features of the carboxyl−carboxylate pairs in *T. reesei* Cel6A are listed in Table 1. It is remarkable that all three carboxyl−carboxylate pairs are located in, or close to, the flexible loop regions that cover the active site tunnel of Cel6A (Figure 2).

Design of the Carboxyl−Carboxylate Pair Mutants. To study the role and function of the carboxyl−carboxylate pairs in *T. reesei* Cel6A, two mutant proteins were constructed. In the first mutant, one carboxyl−carboxylate pair E107-E399 was replaced with a corresponding amide−carboxylate pair Q107-E399 (Cel6A E107Q mutant), and in the second mutant all three carboxyl−carboxylate pairs were mutated in a similar manner (Cel6A E107Q/D170N/D366N mutant). The exchange of a carboxyl−carboxylate pair to an amide−carboxylate pair was predicted to lead to increased stability of the mutant proteins at alkaline pH. The replacement of a carboxylic acid with the corresponding isosteric amide is supposed to cause very little structural distortion to the protein as the amine group probably occupies the position of the protonated oxygen of the original acid in the wild-type. In addition, the following rationales were used to decide which of the residues in a carboxyl−carboxylate pair should be mutagenized to the corresponding amide. For the carboxyl−carboxylate pair E107-E399, the mutation E107Q was

Family 6 enzyme[a]	Organism	I[b] 107[c]	399	II 170	184	III 366	419	IV 146	208	pH range[d]/opt.	Reference
Low pH:											
1QK2 (Cel6A)*	*T. reesei*	E	E	D	E	D	D	E	E	2-9 / 5.0	Koivula *et al.*(*14*)
P46236(GUNB_FUSOX)	*F. oxysporum*	E	E	D	E	D	D	E	N	? / 4.5	Christakopoulos *et al.*(*38*)
P49075(GUX3_AGABI)	*A. bisporus*	E	E	D	E	D	D	G	Q	? / 5.0?	Chow *et al.*(*39*)
Q12646(CELA)	*N. patriciarum*	E	E	M	-	T	D	A	S	4.5 - 6.5 / 5.0	Denman *et al.* (*40*)
Q9UW10(CelcdN'C')	*P. rhizinflata*	E	E	M	-	T	D	P	Q	4 - 8 / 5.5	Liu *et al.* (*41*)
P78721(CelC)	*Orpinomyces* PC-2	E	E	M	-	T	D	A	-	4.6-7.0 / 6.0	Li *et al.* (*42*)
P78720(CelA)	*Orpinomyces* PC-2	E	E	M	-	T	D	P	Q	4.3-6.8 / 5.0	Li *et al.* (*42*)
High pH:											
1BVW (CBHII)*	*H. insolens*	E	E	D	E	H	D	V	S	3 - 11 / 9.0	Schülein (*43*)
1TML (E2)*	*T. fusca*	W	E	N	-	E	-	D	-	4 - 10 / 7.0	Wolfgang & Wilson (*44*)
1DYS (EGII)*	*H. insolens*	K	E	N	E	Q	-	D	A	4.5 - 11 / 7.0	Schülein (*43*)
P50401(CbhA)	*C. fimi*	S	E	D	E	A	G	F	N	? / 7.0	Stålbrand *et al.*(*45*)
Q60029(E3)	*T. fusca*	-	E	N	E	N	G	R	D	6.0 - 10.0 / 8.0	Zhang *et al.*(*46*)

[a] Swiss-Prot or PDB accession number and the name of the enzyme used in the article.
[b] Carboxyl-carboxylate pair number.
[c] Amino acid number in *T. reesei* Cel6A.
[d] The pH range and optimum was taken from the reference. In some cases, indicated with a question mark, only limited information concerning the pH behavior is given in the reference.

FIGURE 3: Sequence alignment showing the conservation of the four carboxyl−carboxylate pairs of *T. reesei* Cel6A in different glycosidases (endoglucanases and cellobiohydrolases) of family 6. The enzymes are grouped into two classes according to their published pH optima. The numbering of the carboxyl−carboxylate pairs is according to the amino acid sequence of *T. reesei* Cel6A. The conserved catalytic carboxyl−carboxylate pair is not included in the comparison. The proteins marked with * are aligned based on their 3-D structures using STAMP (*35*), whereas the rest has been aligned by multiple sequence alignment using ClustalW (*36*−*46*). Only sequences with more than 30% sequence identity to *T. reesei* Cel6A over at least 300 amino acids have been considered.

suggested because E399 is involved in substrate binding and is highly conserved in the family 6 cellulases (Figure 3). In the D170-E184 pair, D170 was mutated to asparagine because the oxygen of E184 (which is involved in the hydrogen bond to D170) also interacts with the L139 backbone nitrogen. An amide in position 184 could not maintain this hydrogen bond and would probably force the side chain in a new conformation. This carboxyl−carboxylate pair is conserved in most of the family 6 cellobiohydrolases listed in Figure 3. In the D366-D419 pair, both side chains show only interactions with water molecules. Here, the decision was made for the exchange D366N because we expected an energetically more favorable geometry of the resulting amide−carboxylate pair (G. Wohlfahrt, manuscript in preparation). For this pair some conservation is observed, but, for example, in *H. insolens* Cel6A (CBHII) the residue corresponding to D366 is changed to histidine, and in *T. fusca* Cel6B (E3) the carboxyl−carboxylate pair is changed to asparagine and glycine (Figure 3).

pH-Dependent Stability of the Cel6A Wild-Type and Mutant Enzymes. To investigate the effect of the mutations on the stability, both guanidinium hydrochloride and temperature-induced unfolding of the purified wild-type and the mutants E107Q and E107Q/D170N/D366N of Cel6A were measured at different pH values. Figure 4 shows the GuHCl induced unfolding curves at pH = 6 (A) and pH = 8 (B) measured by determining the change in tryptophan fluorescence upon unfolding. The two pH values were chosen to correlate protein stability and enzymatic activity, as *T. reesei* Cel6A wild-type is most active at pH 4−6, with rapidly declining activity at and beyond pH 8 (*14*). The unfolding curves at pH 6 resemble those observed for a single transition two-state unfolding reaction, but at pH 8 the curves look more complex for all three enzyme variants (Figure 4). The reversibility of the GuHCl induced unfolding of Cel6A was also tested, but in all cases unfolding was irreversible and thus did not allow analysis of the data using a simple equilibrium two-state unfolding reaction model. As can be seen from the unfolding curves (Figure 4A), the Cel6A wild-type enzyme (□) is somewhat more stable at pH 6 than the carboxyl−carboxylate pair mutants Cel6A E107Q (○) and Cel6A E107Q/D170N/D366N (◇). At pH 8, the order of the relative stabilities is reversed, that is, both the E107Q (○) and the E107Q/D170N/D366N (◇) mutants are more stable than the wild-type enzyme (shown in Figure 4B (□)).

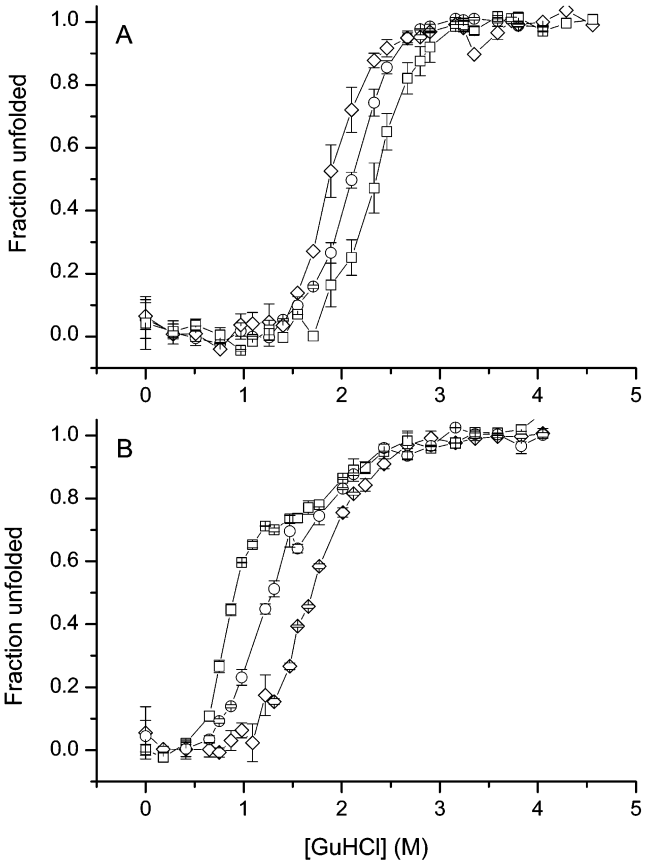

FIGURE 4: GuHCl induced unfolding of Cel6A wild-type and the two carboxyl−carboxylate pair mutants at pH 6 (A) and pH 8 (B). The experimental conditions are described in the Experimental Procedures. Cel6A wild-type (□); Cel6A E107Q mutant (○); and Cel6A E107Q/D170N/D366N mutant (◇).

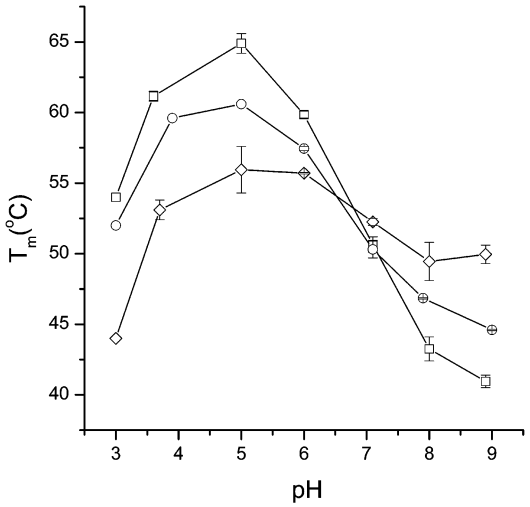

FIGURE 5: Unfolding temperatures (T_m) of Cel6A wild-type and the two carboxyl−carboxylate pair mutants as a function of pH, measured using intrinsic tryptophan fluorescence (excitation wavelength = 280 nm, emission wavelength = 340 nm, bandwidth = 5 nm(ex), 5 nm(em)). The enzyme concentration was 0.5 μM. Samples were heated gradually up to 80 °C, and emission intensity at 340 nm was recorded after every 0.5 °C. The unfolding temperature (T_m) of the different enzymes was determined by the culmination point of the unfolding curves at different pH values. The unfolding of the three enzymes (in the whole pH range studied) was not completely reversible and thus did not allow calculation of the thermodynamic constants. All points (except pH 3) were measured at least as duplicates. Cel6A wild-type (□); Cel6A E107Q mutant (○); and Cel6A E107Q/D170N/D366N mutant (◇).

Overall, the triple mutant (◇) seems to be only slightly destabilized at pH 8 when compared with the measurement at pH 6, while the wild-type enzyme is clearly destabilized at pH 8.

This trend of an increased stability of the mutants at alkaline pH as compared to the wild-type enzyme was further investigated with temperature-induced unfolding monitored using both tryptophan fluorescence and circular dichroism spectroscopy. The fluorescence intensity was monitored at a pH range from 3 to 9. Figure 5 shows the unfolding temperatures (T_m) of the wild-type Cel6A (□) and the two carboxyl−carboxylate pair mutants, Cel6A E107Q (○) and Cel6A E107Q/D170N/D366N (◇), plotted as a function of pH. These stability measurements show a higher unfolding temperature (T_m) for both mutants at alkaline pH (above pH 7) as compared to the Cel6A wild-type enzyme and confirm the results obtained when unfolding was induced with GuHCl (Figure 4). The stabilization by the mutations is highest for the triple mutant (◇), but also the single mutant (○) is more stable than the wild-type under these conditions. At the highest pH measured (pH 8.9), the triple mutant has an about 8 °C and the single mutant an about 3 °C higher T_m as compared to the wild-type enzyme. At acidic pH, the mutations have the reverse effect on the enzyme's stability (i.e., the wild-type enzyme is more stable than the two mutant enzymes; the effect being strongest in the pH range from 3 to 5). In both alkaline and acidic pH regions, the carboxyl−carboxylate pairs would seem to have an additive effect in destabilizing and stabilizing, respectively, the Cel6A fold (Figure 5).

Next, the secondary structure content of all three enzyme variants was monitored at pH 6.1 and 7.9 with CD spectroscopy using a temperature scan. At pH 6.1, both the

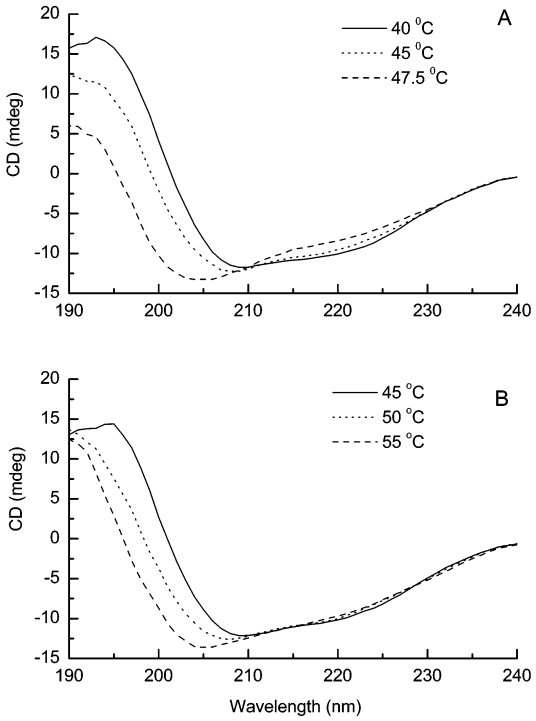

FIGURE 6: Three different CD spectra of the Cel6A wild-type (A) and the Cel6A E107Q/D170N/D366N mutant (B) measured at pH 7.9. The three different spectra show in both cases scans where the protein is fully folded, partially folded, and fully unfolded. As can be seen from the legends, the temperatures where these three spectra were recorded are lower for the Cel6A wild-type enzyme (A) as compared to the triple mutant (B). The experimental conditions are described in the Experimental Procedures.

carboxyl−carboxylate pair mutants show decreased heat stability as compared to the wild-type enzyme (data not shown). At pH 7.9 an inverse effect is seen (i.e., the heat stabilization induced by the single and triple mutations could be observed by CD spectroscopy). Figure 6 shows three different CD spectra of the Cel6A wild-type and the triple mutant at pH 7.9. The three temperature scans shown have been chosen on the basis of the results; the first being in both cases the temperature, where the enzyme is still in its fully folded (native) form, the second where the unfolding starts, and the third where the enzyme is fully unfolded. The first, native spectrum in both cases (Figure 6A,B) shows minima around 209 and 220 nm, which are typical for proteins with a significant amount of α-helical structure (*31*). As can be seen from Figure 6A, the spectrum of the Cel6A wild-type enzyme starts to change above 40 °C (Figure 6A). At 47.5 °C a spectrum with a minimum shifted to 204 nm, typical for an unfolded protein that consists mainly of random coil structure, is observed for Cel6A wild-type, and no further changes in the spectrum are seen when the temperature was raised further. For the triple mutant, the change (unfolding) starts to show above 45 °C, and the protein is fully unfolded only at 55 °C (Figure 6B) (i.e., at a temperature that is approximately 7−8 °C higher than observed with the wild-type enzyme). This increase in the unfolding temperature for the triple mutant seems to correlate well with the increase in the T_m value, measured using tryptophan fluorescence.

Kinetic Characterization and Thermal Inactivation of the Carboxyl−Carboxylate Pair Mutants at Elevated Temperature. The unfolding studies described above demonstrate that both carboxyl−carboxylate pair mutants are more stable

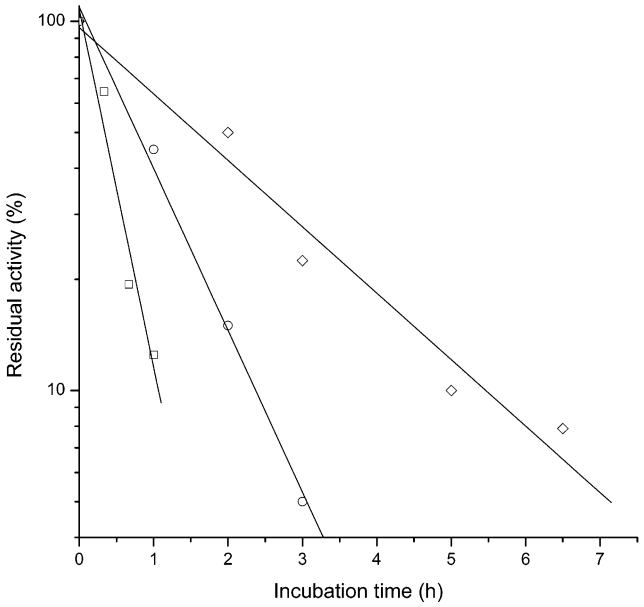

FIGURE 7: Half-life time measurements of the Cel6A wild-type and the two carboxyl−carboxylate pair mutants at 44 °C, pH 7.7. The figure shows a semilogarithmic plot of the residual activity on cellotetraose as a function of incubation time. Activity was normalized to 100% at zero time for each enzyme. Cel6A wild-type (□); Cel6A E107Q mutant (○); and Cel6A E107Q/D170N/D366N mutant (◇).

at alkaline pH when compared to the Cel6A wild-type enzyme (Figures 4−6). The kinetic behavior of the mutants was then studied using cellotetraose (Glc_4) as the substrate. The turnover numbers for the Glc_4 hydrolysis were determined at different pH values from pH 5 to 9. On the basis of the unfolding temperature (T_m) measurements (shown in Figure 5), 44 °C was chosen as the hydrolysis temperature for these experiments. The results (data not shown) show for all three cases pH curves with maximum activity at pH 5 and a clear activity drop between pH 6 and 7 to about 30% of the maximal activity. The absolute turnover number for the triple mutant is slightly decreased (to 60−70%) at acidic and neutral pH (pH 5−7), whereas the single mutant shows basically similar activity as the wild-type enzyme. This drop in the activity of the triple mutant under pH 7 could originate from the lower stability, as amide−carboxylate pairs are expected to be more labile than carboxyl−carboxylate pairs at neutral pH values.

As we were particularly interested in the alkaline pH range, the rates of inactivation were determined at pH 7.7, demonstrating that the half-life time of both mutant enzymes Cel6A E107Q (○) and Cel6A E107Q/D170N/D366N (◇) is increased at pH 7.7, 44 °C (Figure 7). The triple mutant has about 4-fold and the single mutant about 2-fold increased half-life as compared to the wild-type enzyme. On the other hand, the initial catalytic rate (measured at $t = 0$ min) for all three enzyme variants was similar (about 40/min) at this pH.

The increased operational stability of both carboxyl−carboxylate pair mutants was also demonstrated on a more natural substrate, bacterial microcrystalline cellulose (BMCC). The activity of Cel6A wild-type and the two carboxyl−carboxylate pair mutants on BMCC, at pH 7.5 and 44 °C, measured after three different preincubation times, is plotted in Figure 8. As can be seen from Figure 8A (no preincubation), the activity of the two carboxyl−carboxylate pair mutants is about the same or even slightly higher than that of Cel6A wild-type. After 2 h preincubation at pH 7.5 and 44 °C, both mutants Cel6A E107Q (○) and Cel6A E107Q/D170N/D366N (◇) have most of their cellulose degradation activity left (Figure 8B), while the Cel6A wild-type enzyme (□) shows only very low residual activity. Finally, after overnight preincubation at pH 7.5 and 44 °C all three enzymes are practically inactive.

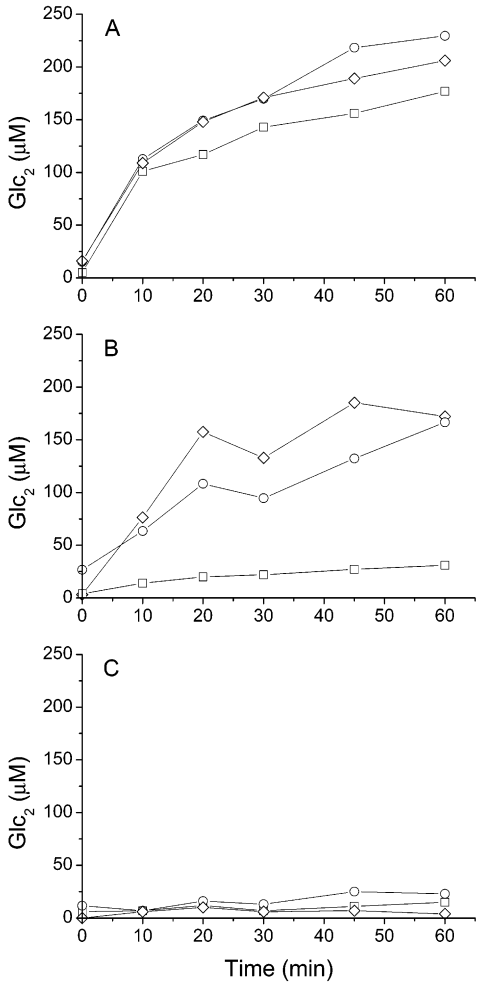

FIGURE 8: Activity of Cel6A wild-type and the two carboxyl−carboxylate pair mutants at 44 °C, pH 7.5 on BMCC, after three different preincubation times. The enzyme preparations (1.9 μM) were preincubated for 0 h (A), 2 h (B), or 21 h (C) at 44 °C, pH 7.5, after which the activity on BMCC (final concentration of 0.7 mg/mL) was measured using the same temperature and pH. Cellobiose (Glc_2) was used as a standard, and the reducing sugars were measured with PAHBAH reagent. Cel6A wild-type (□); Cel6A E107Q mutant (○); and Cel6A E107Q/D170N/D366N mutant (◇).

pH-Dependent Hydrolysis of Insoluble Substrates. Both *Trichoderma* cellobiohydrolases have active sites formed by two or more surface loops enclosing the active site in a tunnel. According to a hypothesis, opening of the active site loops under optimal hydrolysis conditions (pH 4−6) is expected to be a rare event (*7*). On the other hand, the active site loops of *T. reesei* Cel6A have been shown to undergo some conformational changes, which may be needed for full processive activity of the enzyme (*11*, *12*). As all three carboxyl−carboxylate pairs are located in, or close to, the active site loops of Cel6A (Figure 2), repulsion within the

Table 2: Calculated $[Glc_2]/([Glc_1] + [Glc_3])$ Ratios Based on the Soluble Sugars Produced by Cel6A Wild-Type and the E107Q/D170N/D366N Mutant Enzyme on Amorphous Cellulose

enzyme	pH 5[a]	pH 7[a]
Cel6A wild-type	12 ± 1	23 ± 3
Cel6A E107Q/D170N/D366N	10 ± 1	11 ± 2

[a] The $[Glc_2]/([Glc_1] + [Glc_3])$ ratio was determined by following the degradation of amorphous cellulose for 47−52 h using HPLC (see Experimental Procedures) at two different pH values at 27 °C. The $[Glc_2]/([Glc_1] + [Glc_3])$ ratio was measured at 10 different time points, and the average was calculated.

carboxyl−carboxylate pairs at neutral or alkaline pH could lead to conformational changes affecting the activity of the wild-type protein. Owing to more stable interactions, the mutant enzymes should thus be more independent of the pH. To test this, amorphous (i.e., noncrystalline) cellulose was used as a substrate at two different pH values, pH 5 and 7, and the soluble products formed were measured by HPLC. Amorphous cellulose was chosen over crystalline BMCC, as the enzymatic activities are higher on this substrate; thus, more reliable figures for the soluble cello-oligosaccharide (product) concentrations can be obtained. Cel6A wild-type enzyme and the triple mutant E107Q/D170N/D366N were used, and the hydrolysis was followed for 47−52 h at 27 °C taking altogether 10−14 samples at designated time points. The main soluble product formed in all cases was cellobiose, but small amounts of glucose and cellotriose were also produced by both enzymes at both pH values. The triple mutant is slightly more active at pH 5 and clearly more active at pH 7 than the wild-type enzyme throughout the hydrolysis reaction. In addition, both the Cel6A wt and the triple mutant function better at pH 5 than at pH 7 (data not shown). The partial inactivation of Cel6A wt at pH 7 and 27 °C is reversible, as full activity of the wild-type enzyme can be recovered when the enzyme is transferred to pH 5.

The calculated ratios of $Glc_2/(Glc_3 + Glc_1)$ produced on amorphous cellulose are shown in Table 2. This ratio gives an idea about the processivity in terms of consecutive cuts, which the enzymes make along one cellulose chain (*32*). As can be seen in Table 2, the wild-type enzyme shows a 2-fold higher $Glc_2/(Glc_3 + Glc_1)$ ratio at pH 7 when compared to pH 5, while there is basically no pH dependency observed for the triple mutant. Thus, the action of the triple mutant is not pH dependent in a similar manner as that of the wild-type enzyme, possibly because of the fact that amide−carboxylate pairs do not change their protonation state between pH 5 and 7. Furthermore, removal of the three carboxyl−carboxylate pairs leads to an apparently more active enzyme at pH 7 (at 27 °C). On the other hand, the activity decrease of the Cel6A wild-type enzyme at pH 7 seems to be connected to an increased $Glc_2/(Glc_3 + Glc_1)$ ratio. It is tempting to speculate that the apparent increase in processivity is due to local changes in the loop conformation, leading to faster release of the product, cellobiose, after the bond cleavage.

Potential Applications of Carboxyl−Carboxylate Pair Engineering. Carboxyl−carboxylate pairs offer interesting possibilities for the rational engineering of different types of proteins. First, as demonstrated in this article, a protein, which is unstable at high pH values, can be stabilized by replacing its carboxyl−carboxylate pairs (e.g., by amide−carboxylate pairs). This application might be of limited general use as carboxyl−carboxylate pairs do not seem to occur very frequently in proteins (∼19% of known nonredundant structures; G. Wohlfahrt, manuscript in preparation). However, for the examples where they exist (such as *Trichoderma* cellulases) this is a promising approach for this so far unsolved problem. The second potential usage of carboxyl−carboxylate pair engineering would be in stabilizing proteins at low and medium pH values by introducing carboxyl−carboxylate pairs. As seen here, the *T. reesei* Cel6A wild-type enzyme (with carboxyl−carboxylate pairs) was the most stable protein at acidic pH range when compared to the two mutant proteins (with amide−carboxylate pairs). This supports the hypothesis that hydrogen bonds between two carboxylic acids are stronger than, for example, amide−acid hydrogen bonds giving more stability to the protein fold at acidic pH. Additionally, by introducing carboxyl−carboxylate pairs, inactivation of the protein by protonation of the stabilizing carboxylic acids could be shifted to much lower pH. Because of the universal occurrence of amide−acid and amide−amide hydrogen bonds in proteins (in ∼76% of known structures; G. Wohlfahrt, manuscript in preparation), the introduction of carboxyl−carboxylate pairs for stabilization would be possible for a large amount of different proteins that are used in enzyme-catalyzed processes at low or neutral pH values (e.g., various starch processing enzymes and pectinases) (*33*, *34*). A third potential use would be to have pairs of carboxylic acid side chains acting as molecular switches in proteins. Because of the side-chain repulsion occurring at neutral to alkaline pH values, carboxyl−carboxylate pairs could be used as pH-dependent molecular switches either between two protein domains or within one protein domain, where the function (e.g., binding) is modified through carboxyl−carboxylate pairs in a pH-dependent manner.

CONCLUSION

Our results demonstrate that it is possible to affect the stability of a protein at neutral and alkaline pH by mutating carboxyl−carboxylate pairs, which are forming hydrogen bonds with each other, into amide−carboxylate pairs. Furthermore, the effect of the mutations seems to be additive as the stabilization was stronger in the Cel6A triple mutant where three carboxyl−carboxylate pairs were replaced. The increased stability at high pH was reflected as increased activity on insoluble substrates both at 27 and at 44 °C when longer reaction times (>1 h) were used. These results demonstrate that both stability and catalytic activity should be considered if one wants to create an enzyme with optimal activity at a more alkaline pH. Additionally, decreased stability of the mutant enzymes was observed at low pH values suggesting that carboxyl−carboxylate interactions (in Cel6A wild-type) are stronger than those of amide−carboxylate pairs (in mutant enzymes). Hence, introduction of carboxyl−carboxylate pairs is suggested to lead to improved stability at an acidic (and neutral) pH range in general. Overall, carboxyl−carboxylate pair engineering should contribute significantly to rational protein design.

ACKNOWLEDGMENT

We thank Sanna Auer and Tiina Kinnari for their help in cloning, *Trichoderma* transformation, and cultivation work.

Tiina Liljankoski and Riitta Suihkonen are thanked for skillful technical assistance, and Matti Siika-aho is thanked for providing Cel6A wt enzyme preparation.

REFERENCES

1. Sanchez-Ruiz, J. M., and Makhatadze, G. I. (2001) *Trends Biotechnol. 19*, 132−135.
2. Sawyer, L., and James, M. N. G. (1982) *Nature 295*, 79−80.
3. Berman, H. M., Westbrook, J., Feng, Z., Gilliland, G., Bhat, T. N., Weissig, H., Shindyalov, I. N., and Bourne, P. E. (2000) *Nucleic Acids Res. 28*, 235−242.
4. Flocco, M. M., and Mowbray, S. L. (1995) *J. Mol. Biol. 254*, 96−105.
5. Mortensen, U. H., and Breddam, K. (1994) *Protein Sci. 3*, 838−842.
6. Cleland, W. W., Frey, P. A., and Gerlt, J. A. (1998) *J. Biol. Chem. 273*, 25529−25532.
7. Teeri, T. T. (1997) *Trends Biotech. 15*, 160−167.
8. Rouvinen, J., Bergfors, T., Teeri, T. T., Knowles, J. K., and Jones, T. A. (1990) *Science 249*, 380−386.
9. Divne, C., Ståhlberg, J., Reinikainen, T., Ruohonen, L., Pettersson, G., Knowles, J. K. C., Teeri, T. T., and Jones, T. A. (1994) *Science 265*, 524−528.
10. Barr, B. K., Wolfgang, D. E., Piens, K., Claeyssens, M., and Wilson, D. B. (1998) *Biochemistry 37*, 9220−9229.
11. Zou, J., Kleywegt, G. J., Stahlberg, J., Driguez, H., Nerinckx, W., Claeyssens, M., Koivula, A., Teeri, T. T., and Jones, T. A. (1999) *Structure Fold. Des. 7*, 1035−1045.
12. Koivula, A., Ruohonen, L., Wohlfahrt, G., Reinikainen, T., Teeri, T. T., Piens, K., Claeyssens, M., Weber, B.,Vasella, A., Becker, D., Sinnott, M. L., Zou, J., Kleywegt, G., Szardenings, M., Ståhlberg, J., and Jones, T. A. (2002) *J. Am. Chem. Soc. 124*, 10015−10024.
13. Coutinho, P. M., and Henrissat, B. (1999) in *Recent Advances in Carbohydrate Bioengineering* (Gilbert, H. J., Davies, G., Henrissat, B., and Svensson, B., Eds.) pp 3−12, The Royal Society of Chemistry, Cambridge, UK.
14. Koivula, A., Reinikainen, T., Ruohonen, L., Valkeajärvi, A., Claeyssens, M., Teleman, O., Kleywegt, G., Szardenings, M., Rouvinen, J., Jones, T. A., and Teeri, T. T. (1996) *Protein Eng. 9*, 691−699.
15. Mach, R. L., Schindler, M., and Kubicek, C. P. (1994) *Curr. Genet. 6*, 567−570.
16. Ståhlberg, J., Divne, C., Koivula, A., Piens, K., Claeyssens, M., Teeri, T. T., and Jones, T. A. (1996) *J. Mol. Biol. 264*, 337−349.
17. Srisodsuk, M., Reinikainen, T., Penttilä, M., and Teeri, T. T. (1993) *J. Biol. Chem. 268*, 20756−20761.
18. Reinikainen, T., Henrikson, K., Siika-aho, M., Teleman, O., and Poutanen, K. (1994) *Enzyme Microbiol. Technol. 17*, 888−892.
19. Tomme, P., McRae, S., Wood, T. M., and Claeyssens, M. (1988) *Methods Enzymol. 160*, 187−192.
20. Laemmli, U. K. (1970) *Nature 227*, 680−685.
21. Towbin, H., Staehelin, T., and Gordon, J. (1979) *Proc. Natl. Acad. Sci. U.S.A. 76*, 4350−4354.
22. Koivula, A., Lappalainen, A., Virtanen, S., Mäntylä, A. L., Suominen, P., and Teeri, T. T. (1996) *Protein Exp. Purif. 8*, 391−400.
23. Aho, S., Olkkonen, V., Jalava, T., Paloheimo, M., Bühler, R., Niku-Paavola, M., Bamford, D. H., and Korhola, M. (1991) *Eur. J. Biochem. 200*, 643−649.
24. Teleman, A., Koivula, A., Reinikainen, T., Valkeajärvi, A., Teeri, T. T., Drakenberg, T., and Teleman, O. (1995) *Eur. J. Biochem. 231*, 250−258.
25. Gilkes, N. R., Jervis, E., Henrissat, B., Tekant, B., Miller, R., Jr., Warren, A., and Kilburn, D. G. (1992) *J. Biol. Chem. 267*, 6743−6749.
26. Boer, H., Teeri, T. T., and Koivula, A. (2000) *Biotech. Bioeng. 69*, 486-494.
27. Isogai, A., and Atalla, R. H. (1990) *J. Polym. Sci., Part A: Polym. Chem. 29*, 113−119.
28. Eftink, M. R. (1995) *Methods Enzymol. 259*, 487−512.
29. Pace, C. N. (1986) *Methods Enzymol. 131*, 266−280.
30. Nozaki, Y. (1972) *Methods Enzymol. 26*, 43−50.
31. Alder, A. J., Greenfield, N. J., and Fasman, G. D. (1973) *Methods Enzymol. 27*, 675−735.
32. Pagès, S., Kester, H. C., Visser, J., and Benen, J. A. (2001) *J. Biol. Chem. 276*, 33652−33656.
33. Kennedy, J. F., Cabalda, V. M., and White, C. A. (1988) *TIBTECH 6*, 184−189.
34. Kashyap, D. R., Vohra, P. K., Chopra, S., and Tewari, R. (2001) *Biores. Technol. 77*, 215−227.
35. Russell, R. B., and Barton, G. J. (1992) *Proteins 14*, 309−323.
36. Thompson, J. D., Higgins, D. G., and Gibson, T. J. (1994) *Nucleic Acids Res. 22*, 4673−4680.
37. Mizuguchi, K., Deane, C. M., Blundell, T. L., Johnson, M. S., and Overington, J. P. (1998) *Bioinformatics 14*, 617−623.
38. Christakopoulos, P., Kekos, D., Macris, B. J., Claeyssens, M., and Bhat, M. K. (1995) *Arch. Biochem. Biophys. 316*, 428−433
39. Chow, C., Yague, E., Raguz, S., Wood, D. A., and Thurston, C. F. (1994) *Appl. Environ. Microbiol. 60*, 2779−2785.
40. Denman, S., Xue, G. P., and Patel, B. (1996) *Appl. Environ. Microbiol. 62*, 1889−1896.
41. Liu, J., Tsai, C., Liu, J., Cheng, K., and Cheng, C. (2001) *Enzyme Microbiol. Technol. 28*, 582−589.
42. Li, X. L., Chen, H., and Ljungdahl, L. G. (1997) *Appl. Environ. Microbiol. 63*, 4721−4728.
43. Schulein, M. (1997) *J. Biotechnol. 57*, 71−81.
44. Wolfgang, D. E., and Wilson, D. B. (1999) *Biochemistry 38*, 9746−9751.
45. Stålbrand, H., Mansfield, S. D., Saddler, J. N., Kilburn, D. G., Warren, R. A., and Gilkes, N. R. (1998) *Appl. Environ. Microbiol. 64*, 2374−2379.
46. Zhang, S., Lao, G., and Wilson, D. B. (1995) *Biochemistry 34*, 3386−3395.

BI034954O